Graphical Data Display for Clinical Cardiopulmonary Exercise Testing

Daniel Dumitrescu and Stephan Rosenkranz

Klinik III für Innere Medizin, Herzzentrum der Universität zu Köln, Cologne, Germany

Abstract

Cardiopulmonary exercise testing is a well-known, valuable tool in the clinical evaluation of patients with different causes of exercise limitation and unexplained dyspnea. A wealth of data is generated by each individual test. This may be challenging regarding a comprehensive and reliable interpretation of an exercise study in a timely manner. An optimized graphical display of exercise data may substantially help to improve the efficacy and reliability of the interpretation process. However, there are limited and heterogeneous recommendations on standardized graphical display in current exercise testing guidelines. To date, a widely used three-by-three array of specifically arranged graphical panels known as the "nine-panel plot" is probably the most common method of plotting exercise gas exchange data in a standardized way. Furthermore, optimized scaling of the plots, the use of colors and style elements, as well as suitable averaging methods have to be considered to achieve a high level of quality and reproducibility of the results. Specific plots of key parameters may allow a fast and reliable visual determination of important diagnostic and prognostic markers in cardiac and pulmonary diseases.

Keywords: cardiopulmonary exercise testing; formatting; graphical display; nine-panel plot

(Received in original form December 4, 2016; accepted in final form May 25, 2017)

Correspondence and requests for reprints should be addressed to Daniel Dumitrescu, M.D., Klinik III für Innere Medizin, Herzzentrum der Universität zu Köln, Kerpener Str. 62, 50937 Köln, Germany. E-mail: daniel.dumitrescu@uk-koeln.de

Ann Am Thorac Soc Vol 14, Supplement 1, pp S12–S21, Jul 2017

DOI: 10.1513/AnnalsATS.201612-955FR
Internet address: www.atsjournals.org

Cardiopulmonary exercise testing (CPET) is a well-known, valuable tool in the clinical evaluation of patients with different causes of exercise limitation and/or unexplained dyspnea. The wealth of data that is generated during CPET is a major asset of the method, as it allows a comprehensive view of the metabolic changes at rest and during exercise. At the same time, this wealth of data is a significant challenge in terms of selection, display, management, and interpretation of the obtained data.

Although the determination of the anaerobic threshold (AT, termed VT_1 in the German literature) and of key parameters at peak exercise are essential for a meaningful interpretation of a test, only the continuous graphical display of resting, exercise, and recovery data is able to visualize dynamic changes in metabolism and to demonstrate pathophysiological changes that may not be visible at rest or at lower exercise levels. As CPET is a diagnostic tool that reveals dynamic processes during exercise, a visual interpretation of the obtained data is mandatory.

Despite numerous guidelines and recommendations on the use of CPET, there is only limited and heterogeneous advice on the graphical display of the obtained data. Optimization and standardization of the visual data plotting and highlighting of key parameters will help to improve the reliability, interpretation, and reproducibility of test results, and the clinical use and acceptance of this important diagnostic test.

Existing Recommendations on Exercise Testing and Graphical Display

The first reports of online breath-by-breath measurement systems and a reliable graphical display of the data were reported in the 1970s (1). Over the years, enormous advances in computer technology have expanded the possibilities of data acquisition and display. Textbooks and a large number of major medical societies involved in the clinical management of cardiac or respiratory diseases have published recommendations on clinical exercise testing (2–14). Table 1 gives an overview of available exercise testing guidelines, starting from 1997. Only a part of these publications include specific recommendations for the graphical display of exercise data. Furthermore, these recommendations are heterogeneous regarding graphs, axes, and number of panels.

Data Processing and Averaging Methods

The ability of measuring and storing breath-by-breath data opened new possibilities in the field of CPET. A high data sampling frequency allows the visualization of dynamic processes,

Table 1. Exercise testing recommendations published by selected major medical societies involved in the management of cardiac or respiratory diseases

Year Published	Source	Focus	Recommendations on Graphical Display
1997 (3)	American College of Cardiology/American Heart Association	Cardiovascular diseases	Visual determination of the anaerobic threshold
1997 (4)	European Respiratory Society	Lung diseases	Basic plots in 8 panels: oxygen uptake on the *x-axis* in most panels Visual determination of the anaerobic threshold
2000 (5)	American College of Cardiology/ American Heart Association	Clinical competence statement	Gas exchange measurements only mentioned in relation to pediatric exercise testing; no advice on graphical display
2002 (6)	American College of Cardiology/ American Heart Association	Cardiovascular diseases: update on the 1997 Exercise Testing Guidelines (3)	No specific advice on graphical display
2003 (7)	American Thoracic Society/ American College of Chest Physicians	Clinical indications, standardization issues, interpretative strategies	Visual determination of the anaerobic threshold Flow–volume loops during exercise Basic plots in 9 panels: oxygen uptake on the *x-axis* in most panels
2007 (8)	European Respiratory Society	Assessment of exercise intolerance Prognostic assessment Evaluation of therapeutic interventions	No specific recommendations on graphical display
2009 (9)	European Association for Cardiovascular Prevention and Rehabilitation/European Society of Cardiology	Functional evaluation of cardiac patients	Visual determination of the anaerobic threshold Determination of the oxygen uptake efficiency slope Determination of ventilatory efficiency Determination of the oxygen uptake/work rate relationship
2010 (10)	American Heart Association	Comprehensive overview of clinical exercise testing	Visual determination of the anaerobic threshold Graphical display of data is not considered necessary in the final report
2012 (11)	European Association for Cardiovascular Prevention and Rehabilitation/American Heart Association	Exercise data assessment in specific patient populations	Recommended data averaging of a fixed 10-s time frame Recommendations on key exercise parameters, no specific recommendations on graphical display
2016 (12)	European Association for Cardiovascular Prevention and Rehabilitation/American Heart Association	Exercise data assessment in specific patient populations: update of the 2012 recommendations (11)	Flow–volume loops during exercise No additional recommendations compared to (11)

Numbers in parentheses indicate References.

such as oscillatory breathing patterns, within a narrow time frame. On the other hand, a real breath-by-breath sampling rate is associated with the burden of worsened graphical visualization, due to the high density of data points. Thus, the display of the entire breath-by-breath data set is not helpful in most cases, especially with longer test durations. A reasonable method of data averaging has to be performed to optimize the graphical data display. Figure 1 shows the original breath-by-breath recordings as well as the most common methods of data averaging in a maximal incremental test.

Data averaging may be performed either on the basis of a fixed time interval or as a rolling average on the basis of a defined number of breaths. A fixed time frame averages all data points within this time frame. In clinical practice, the most common settings range from 10- to 60-second periods. Rolling averages usually contain units of five to eight breaths. Compared with fixed time frames, the rolling average method is able to achieve an improved smoothing of the displayed curves. However, due to a shortening of single-breath duration at higher exercise levels, the time frame of averaged data points shortens during exercise: at rest, an eight-breath interval (at a rate of 20 breaths/min) spans a time frame of 24 seconds. However, at peak exercise, with high breathing frequencies, the time frame of an eight-breath average may decline below 10 seconds, so that data at peak exercise may become noisy. There are no consistent recommendations among existing guidelines on the averaging method. The optimal selection of an averaging method may be based on the individual situation. Long tests require a longer averaging period than short tests. The interpretation of noisy data may be improved with a rolling average method, whereas short dynamic processes such as oscillatory breathing might be better detected with a short fixed time frame averaging. It is important to be aware that switching the averaging method of a test may significantly alter results such as peak oxygen uptake and the AT (Figure 1). Thus, the averaging method should be documented on the test. For serial measurements, reproducibility increases if only one averaging method is

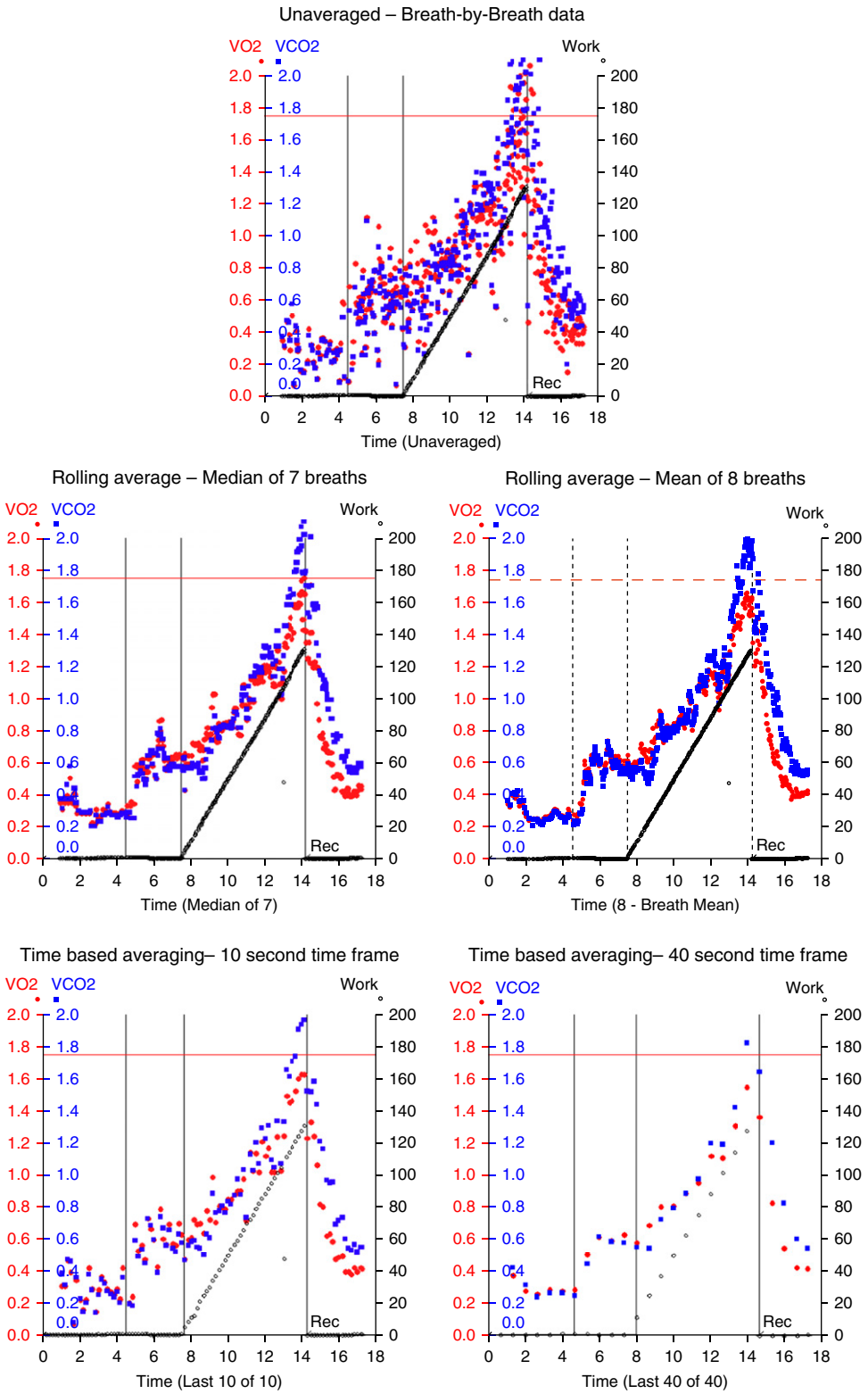

Figure 1. Display of $\dot{V}O_2$ (*red*) (L/min), $\dot{V}CO_2$ (*blue*) (L/min), and work rate (Work, *black*) (W) in a maximal exercise test with an incremental ramp protocol in a healthy female subject. The *vertical lines* indicate, from left to right, the start of the warm-up phase, the start of the incremental phase, and the end of exercise, respectively. The *horizontal red line* displays the predicted oxygen uptake value. On the basis of the breath-by-breath dataset, the same test is displayed with different averaging methods, separated into rolling averaging methods and time-based averaging methods. Note the significant differences in peak $\dot{V}O_2$ and peak $\dot{V}CO_2$, depending on the averaging method. Time is displayed in minutes. Rec = recovery phase.

used in all performed tests for an individual subject.

Specific Considerations for a Standardized Graphical Display

Due to the wealth of parameters obtained by CPET, as well as different averaging methods and graphical aids such as colors, symbol styles, and symbol sizes, there are countless possibilities of plotting test results. Recommendations have been published as part of current guidelines (Table 1) and in textbooks (2, 14). However, these recommendations are heterogeneous. Although this leaves room for individual solutions of an optimized graphical display, heterogeneity likely impairs intra- and interindividual reproducibility of data reading and interpretation. A rational approach toward a standardized, comprehensive graphical output should consider several important aims:

- All relevant test data should be visible on one page.
- From all available parameters and potential combinations, the display should contain a standardized selection of relevant values, to maintain clarity of the graphs. Special plots, if necessary for specific questions, should be added on separate pages.
- The arrangement of the graphical display should follow a specific structure.
- The obtained results should be easily distributable to other colleagues, if necessary, without any loss of information.

Achieving these goals requires the skilled use of graphical elements and sizing and scaling of the graphs. Using a standardized, widely known and accepted selection/arrangement of key parameters such as the nine-panel plot facilitates a reliable, structured interpretation as well as a feasible distribution of test results.

Colors, Symbols, Connector Lines

The use of colors in exercise test graphs is common; however, there is no standardized color coding for gas exchange parameters according to existing guidelines.

For clinical purposes, a specific color coding is of less importance than being able to perform a distinct allocation of parameters in the plotted graphs, even on a black-and-white printout or copy. Thus, the sole use of colored line plots—without showing the original data points—is inferior to the use of

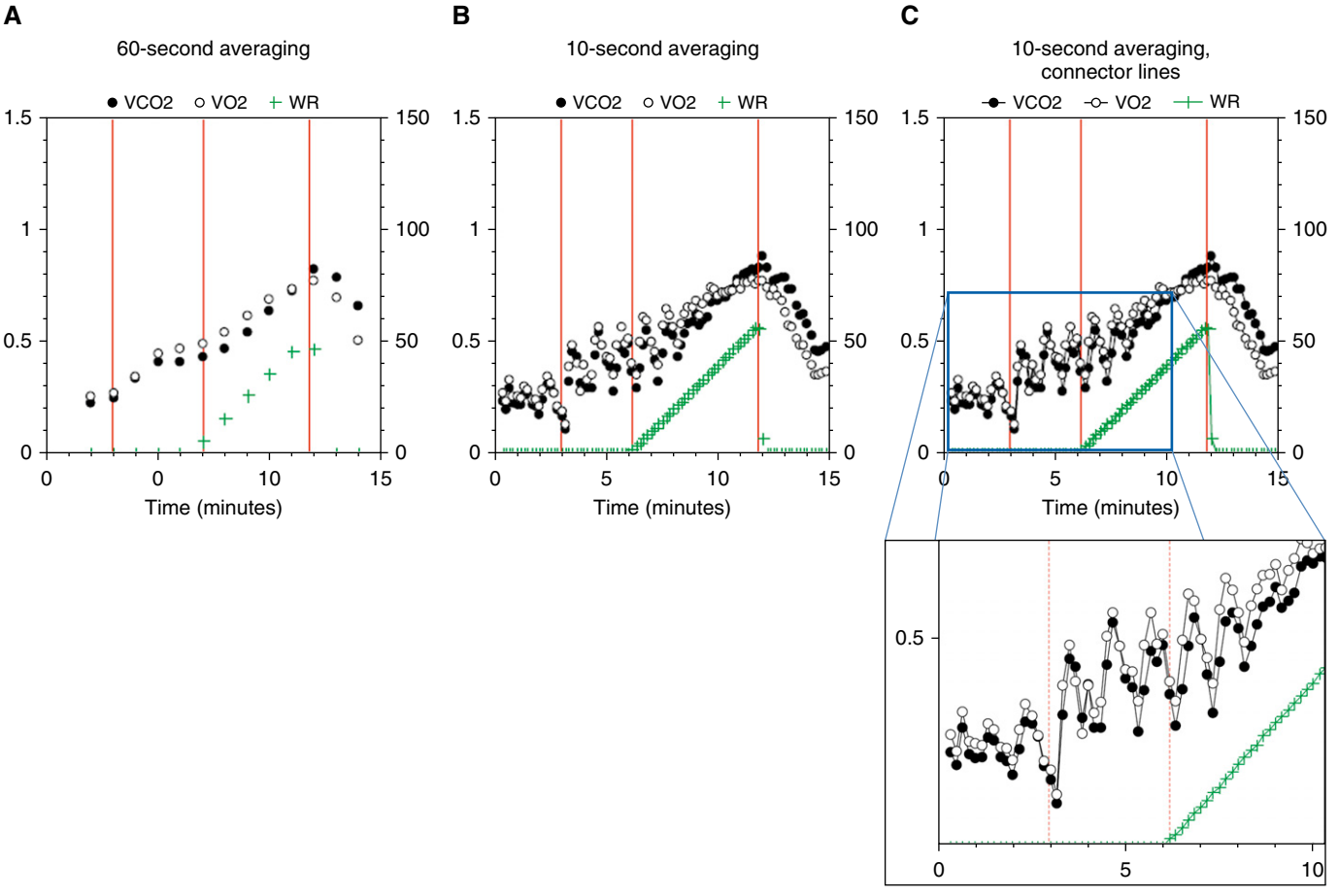

Figure 2. Oscillatory breathing in a patient with left-sided heart failure with reduced ejection fraction. The oscillations are only visible at rest and low-intensity exercise, and they disappear with increasing workload. (*A*) Low density of data points completely hides the oscillatory breathing pattern. (*B*) A higher density of data points (10-s averaging) is better able to show the oscillations. (*C*) Best results are obtained with a high density of data points, connector lines, and magnifying the "area of interest." $\dot{V}O_2$ and $\dot{V}CO_2$ are shown in L/min, work rate in W, and time in minutes. WR = work rate.

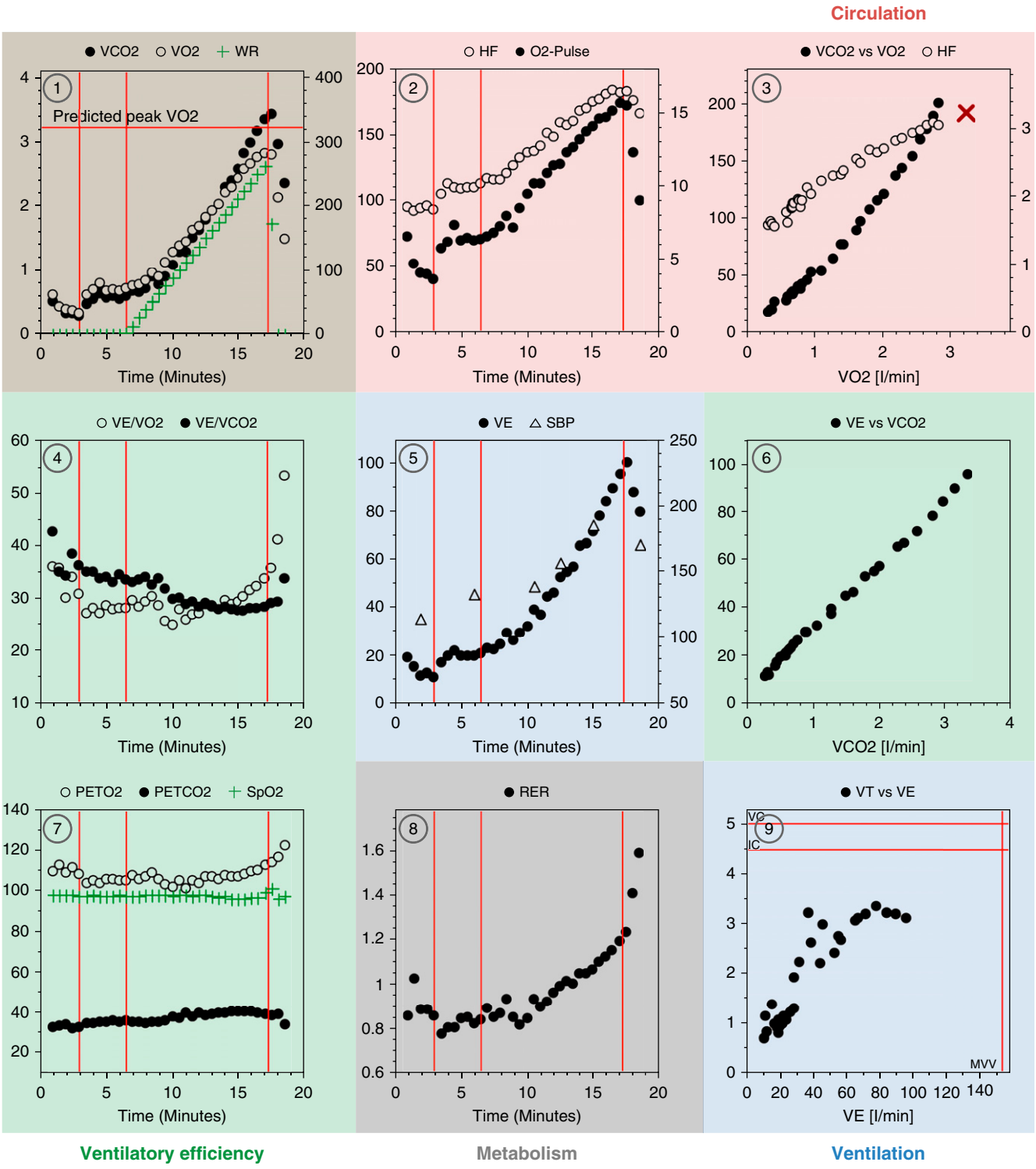

Figure 3. Exercise test of a healthy 28-year-old male subject. Nine-panel plot graphical display according to Reference 14, with a 30-second averaging of the data. *Panels 2* and *3* reflect circulatory parameters (*red area*). *Panels 5* and *9* show ventilatory parameters (*blue areas*). *Panels 4*, *6*, and *7* reflect parameters of ventilatory efficiency (*green areas*). *Panel 8* (respiratory exchange ratio, RER) reflects general metabolic changes (*gray area*). *Panel 1* has a central role (*composite color/brown area*). The *vertical red lines* in *panels 1*, *2*, *4*, *5*, *7*, and *8* indicate, from left to right, the start of the unloaded pedaling phase, the start of the incremental work rate (WR) increase, and the end of the exercise phase, respectively. HF is shown in beats/min; O_2 pulse, ml/beat; $P_{ET_{O_2}}$, $P_{ET_{CO_2}}$, and SBP, mm Hg; Sp_{O_2}, %; $\dot{V}_{CO_2}$, $\dot{V}E$, and $\dot{V}_{O_2}$, L/minl; VT, L; and WR, W. HF = heart rate; IC = inspiratory capacity; MVV = maximal voluntary ventilation; O_2 pulse = $\dot{V}_{O_2}$/heart rate; $P_{ET_{CO_2}}$ = end-tidal carbon dioxide partial pressure; $P_{ET_{O_2}}$ = end-tidal oxygen partial pressure; SBP = systolic blood pressure; Sp_{O_2} = peripheral oxygen saturation.

specifically shaped data points/symbols, either with or without connector lines. The shape of data points should be unique for each parameter on a plot with several variables, and clearly marked in the legend. Connector lines may increase the graphical noise in a plot; however, they might be helpful in recognizing oscillatory breathing patterns. Display examples of oscillatory breathing in a patient with heart failure are shown in Figure 2.

The Nine-Panel Plot

In 1977, the working group lead by Karlman Wasserman was approached by the U.S. Department of Labor with a question related to occupational medicine. A cohort of nearly 400 shipyard workers who had been potentially exposed to asbestos had to be evaluated regarding their exercise capacity. If a reduction in exercise capacity was found, the primary mechanism and a potential relation to asbestos exposure had to be elucidated. The time frame for this evaluation was narrow, so that a fast and reliable method for the evaluation of exercise impairment was required (13). For this project, a visual interpretation of exercise data proved to be superior to a mere numerical analysis of key parameters, especially regarding determination of the primary mechanism of exercise intolerance. This standardized 3 × 3 graphic array display, the nine-panel plot in its first version, was published almost at the same time (2).

This format was extensively used by clinicians worldwide in the following years. To date, the nine-panel plot is still the most common method of standardized clinical exercise test interpretation. Exercise testing guidelines issued by the European Respiratory Society (4) and the American Thoracic Society/American College of Chest Physicians (7) proposed different variations of this plotting method. Due to didactical reasons, the fifth edition of the textbook *Principles of Exercise Testing and Interpretation*, published in 2012, presented a different arrangement of the panels, without altering the content of each single panel (14). An example of a healthy subject (Figure 3) illustrates the didactic concept of the nine-panel plot. Panel 1 shows $\dot{V}O_2$, $\dot{V}CO_2$, and work rate (WR) over time. Predicted peak $\dot{V}O_2$ is plotted as a horizontal line in the panel. In panel 2, heart rate (HR) and oxygen pulse ($\dot{V}O_2$/HR) are plotted over time. Panel 3 shows HR and $\dot{V}CO_2$ plotted over $\dot{V}O_2$. The intersection of predicted peak $\dot{V}O_2$ and predicted HR is marked as "X" in the plot. Panel 4 shows the ventilatory equivalent for O_2 ($\dot{V}E/\dot{V}O_2$) and the ventilatory equivalent for CO_2 ($\dot{V}E/\dot{V}CO_2$) plotted over time. Of note, in contrast to the simple $\dot{V}E/\dot{V}O_2$ and $\dot{V}E/\dot{V}CO_2$ relationship, the ventilatory equivalent for O_2 and for CO_2 requires additional subtraction of (valve dead space × breathing frequency) from $\dot{V}E$. Panel 5 shows $\dot{V}E$ and systolic blood pressure (SBP) plotted as a function of time. In panel 6, $\dot{V}CO_2$ is plotted as a function of $\dot{V}E$. Panel 7 shows end-tidal partial pressures of O_2 (PET_{O_2}) and CO_2 (PET_{CO_2}) as well as peripheral oxygen saturation (Sp_{O_2}) plotted over time. Panel 8 shows the respiratory exchange ratio (RER) plotted as a function of time. Panel 9 shows VT plotted as a function of $\dot{V}E$. Vital capacity (VC) and inspiratory capacity (IC) are shown as horizontal lines. Maximal voluntary ventilation (MVV) is shown as a vertical line in this panel.

Specific Graphs for Visual Test Interpretation

On the basis of the nine-panel plot, selected panels deserve a separate discussion regarding an optimized graphical display. A specific scaling or a specific arrangement within these plots may facilitate a reliable visual determination of important diagnostic and/or prognostic markers.

$\dot{V}O_2$, $\dot{V}CO_2$ (Panel 1)

Oxygen uptake ($\dot{V}O_2$) is one of the most important parameters in terms of diagnostic assessment, and of risk stratification in cardiac and pulmonary diseases. During incremental exercise, $\dot{V}O_2$ increases at a rate of about 10 ml/min/W (15). A lower rate may indicate an impaired oxygen transport and/or circulatory impairment during exercise. $\dot{V}CO_2$ closely correlates with $\dot{V}O_2$ and shows specific patterns below and above the AT. Below the AT, $\dot{V}CO_2$ increases at about the same rate as $\dot{V}O_2$. Above the AT, $\dot{V}CO_2$ increases at a higher rate than $\dot{V}O_2$. During recovery, $\dot{V}CO_2$ decreases less rapidly than $\dot{V}O_2$ in healthy subjects, leading to an abrupt increase in respiratory exchange ratio. Examples of a healthy subject and a patient with severe heart failure are shown in Figure 4. To provide an optimized visual

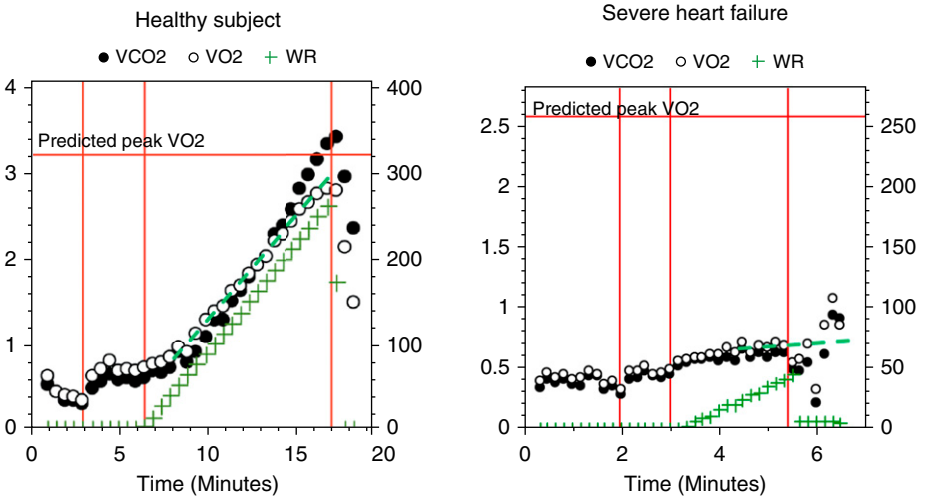

Figure 4. Optimized graphical display of *Panel 1* of Figure 3. $\dot{V}O_2$, $\dot{V}CO_2$, and work rate (WR) are displayed together in this panel. $\dot{V}O_2$ and $\dot{V}CO_2$ (in L/min) are plotted with an identical scaling. $\dot{V}O_2$ and work rate (in W) are plotted with a scaling ratio of 1:100. The *green fitting line* shows the same slope as the WR increase in the healthy subject, indicating a physiological $\dot{V}O_2$ increase of 10 ml/min/W. In contrast, the patient with severe heart failure has a markedly reduced $\dot{V}O_2$/WR increase, so that the slope of the fitting line is dramatically reduced compared with WR increase.

display of this graph, several aspects are important:

- The predicted value of peak $\dot{V}O_2$ should be visually displayed.
- $\dot{V}O_2$ and $\dot{V}CO_2$ should be displayed on an identical scale.
- WR may be included in this panel. As $\dot{V}O_2$ increases with 10 ml/min/W for ergometer work (15), a scaling aspect of 10:1 between $\dot{V}O_2$ and WR reveals whether the slope of 10 ml/min/W is preserved during exercise (Figure 4A), or if the /work rate response is reduced (Figure 4B). If $\dot{V}O_2$ is expressed as liters per minute, the scaling aspect of $\dot{V}O_2$/WR has to be changed to 1:100.

Determination of the AT (Panels 3, 4, 7)

The first and probably best-known publication on the determination of the AT was published in 1986 (16). In this panel, $\dot{V}O_2$ is plotted on the *x-axis* and $\dot{V}CO_2$ is plotted on the *y-axis*, with a scaling aspect of 1:1 (Figure 5A). When anaerobic metabolism occurs, the slope of the $\dot{V}O_2$ versus $\dot{V}CO_2$ graph exceeds a value of 1. With an identical scaling of the *x-axis* and the *y-axis*, a reference line with an angle of 45 degrees (slope = 1) may help to identify this point. The same phenomenon is visualized in a plot of $\dot{V}E/\dot{V}O_2$ over time (Figure 5B), or $P_{ET}O_2$ over time (Figure 5C), as suggested by the European Association for Cardiovascular Prevention and Rehabilitation guidelines (9). The ratio of $\dot{V}E/\dot{V}O_2$, as well as $P_{ET}O_2$, decreases during exercise and reaches a nadir value just below the AT. After the onset of anaerobic metabolism, the $\dot{V}E/\dot{V}O_2$ ratio and $P_{ET}O_2$ start increasing from their nadir values. The AT is expressed as the $\dot{V}O_2$ value at the time point of $\dot{V}E/\dot{V}O_2$ or $P_{ET}O_2$ increase. All methods of AT determination should lead to an equal result.

HR Response (Panel 3)

In healthy subjects, a linear increase in HR will be observed in a plot of HR (*y-axis*) over $\dot{V}O_2$ (*x-axis*). Furthermore, a fitting curve through the data points will aim at the intersection of the predicted values for $\dot{V}O_2$ and HR (Figure 6A). A reduced HR increase is seen in athletes (Figure 6B) or in patients taking β-blockers. A pronounced reduction of the HR vs $\dot{V}O_2$ slope in

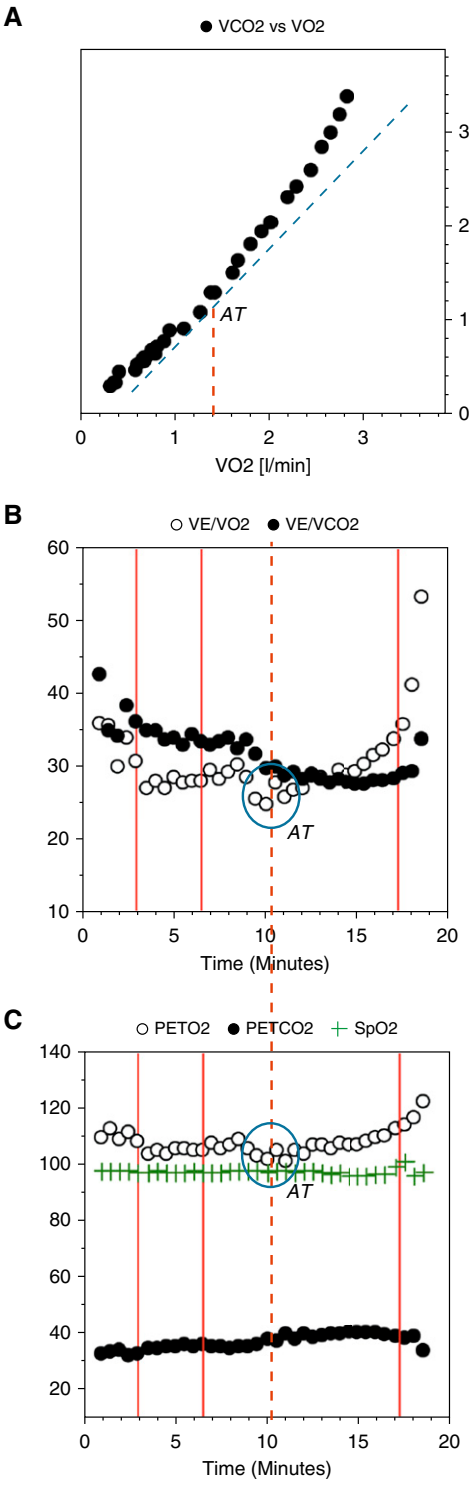

Figure 5. Different methods of determining the anaerobic threshold (AT, termed VT_1 in the German literature). (*A*) V-slope method by Beaver and colleagues (16): $\dot{V}O_2$ and $\dot{V}CO_2$ (in L/min) are plotted with a scaling aspect of 1:1. The AT is determined by drawing a reference line (*blue*) with a slope of 1 (45-degree angle). When the $\dot{V}O_2/\dot{V}CO_2$ slope exceeds a value of 1, the AT has been reached. (*B*) The AT has been reached after the $\dot{V}E/\dot{V}O_2$ relationship has passed its minimum value during exercise and starts increasing (*blue oval*). (*C*) The AT has been reached after the end-tidal oxygen partial pressure ($P_{ET}O_2$) (mm Hg) has passed its minimum value during exercise and starts increasing (*blue oval*). All three methods should correlate. $P_{ET}CO_2$ = end-tidal carbon dioxide partial pressure (mm Hg); Sp_{O_2} = peripheral oxygen saturation (%).

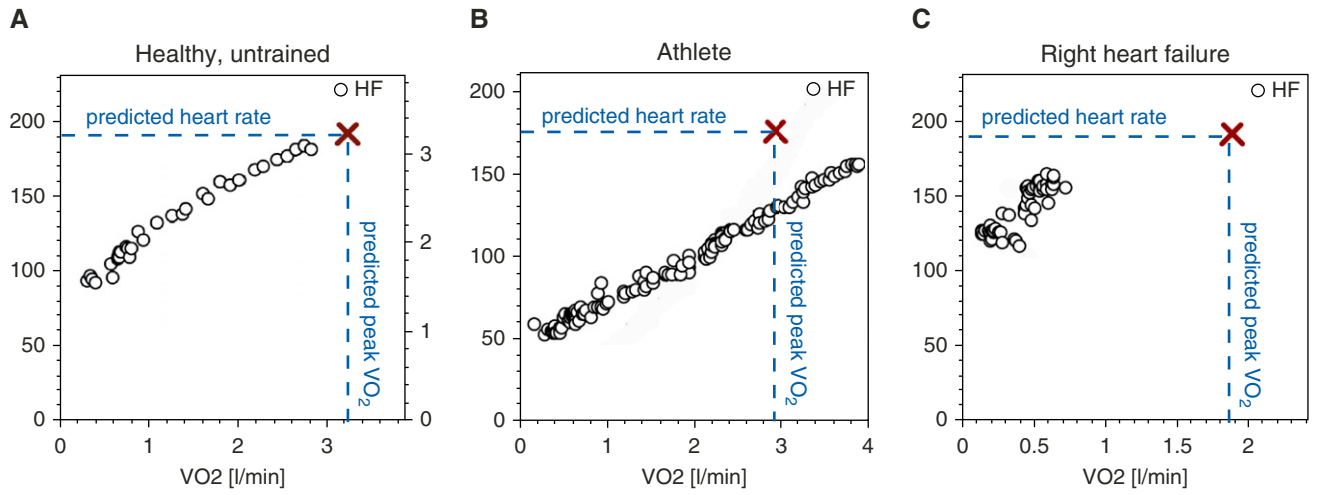

Figure 6. Heart rate (HF; *y-axis*) plotted over $\dot{V}O_2$ (*x-axis*). X (*red*) marks the intersection of predicted heart rate (*horizontal dashed line*) and predicted peak $\dot{V}O_2$ (*vertical dashed line*). (*A* and *B*) Physiological pattern in an athlete and in an untrained subject (linear increase of heart rate vs. $\dot{V}O_2$ with a shallow slope). (*C*) Pathological pattern in a patient with severe right-heart failure (resting tachycardia, steep increase of the heart rate vs. $\dot{V}O_2$ slope).

symptomatic patients may also indicate chronotropic incompetence, which is, for instance, frequently found in patients with heart failure and preserved ejection fraction. If a significant circulatory limitation is present, and a further increase of cardiac output is impaired at a certain exercise level, there is an excess increase of HR, which is also visualized with this plot (Figure 6C).

Ventilatory Efficiency (Panels 4, 6)

For an optimized visualization of ventilatory efficiency, the display of $\dot{V}E$ (*y-axis*) over $\dot{V}CO_2$ (*x-axis*) reveals the relationship between these two parameters during exercise. Under physiological conditions, $\dot{V}E$ tracks $\dot{V}CO_2$ even above the AT. Only close to maximal exercise, lactic acidosis itself becomes an additional chemoreceptor stimulus and causes pronounced hyperventilation (17). This is known as the "respiratory compensation point." Above this point, the linearity between $\dot{V}E$ and $\dot{V}CO_2$ cannot be maintained (Figure 7). The linear part of this plot, below the respiratory compensation point, may be used to calculate the slope of the $\dot{V}E/\dot{V}CO_2$ relationship, which has been validated as a powerful prognostic marker by numerous studies in cardiac and pulmonary diseases.

The $\dot{V}E/\dot{V}CO_2$ slope may be calculated visually from the linear portion of the $\dot{V}E$ versus $\dot{V}CO_2$ plot (Figure 7). Special attention may be given to the *y-axis* intercept of the plot, as this may contain relevant information on dead space ventilation (18–20). This information may also be visualized if the $\dot{V}E/\dot{V}CO_2$ relationship during exercise is plotted over time (Figure 3, Panel 4 in the nine-panel plot). Mathematical considerations suggest that the $\dot{V}E/\dot{V}CO_2$ relationship likely decreases during exercise if the *y-axis* intercept of the $\dot{V}E$ versus $\dot{V}CO_2$ plot is positive (Figure 8A). If the *y-axis* intercept is negative, the $\dot{V}E/\dot{V}CO_2$ relationship will likely increase during exercise (Figure 8B).

Normal Values

The interpretation of exercise data and the detection of pathological exercise gas exchange patterns require an adequate knowledge about normal response patterns to exercise (21). Peak $\dot{V}O_2$ depends on several parameters, such as sex, age, height, and weight. Peak $\dot{V}O_2$, AT, and ventilatory efficiency decrease with age. To date, several reference datasets for key exercise parameters have been published. The two largest datasets have been reported by Wasserman and colleagues (14) and by Gläser and colleagues (22). Thus, documenting the source of predicted value calculation may be of clinical relevance. A detailed overview of reference datasets and the correlation among the different datasets is given in the textbook by Wasserman and colleagues (14).

An integration of predicted values into the graphical display as well as the display of normal response ranges is offered by most manufacturers.

Special Plots

The nine-panel plot may be seen as an approach to have a minimal,

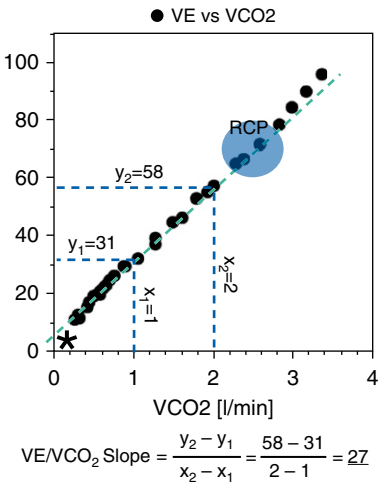

Figure 7. $\dot{V}E$ (*y-axis*) (L/min) plotted over $\dot{V}CO_2$ (*x-axis*). The respiratory compensation point (RCP) becomes visible at high exercise intensity (*blue shaded area*). A manual example calculation is performed for the $\dot{V}E/\dot{V}CO_2$ slope in this case. *Positive *y-axis* intercept value.

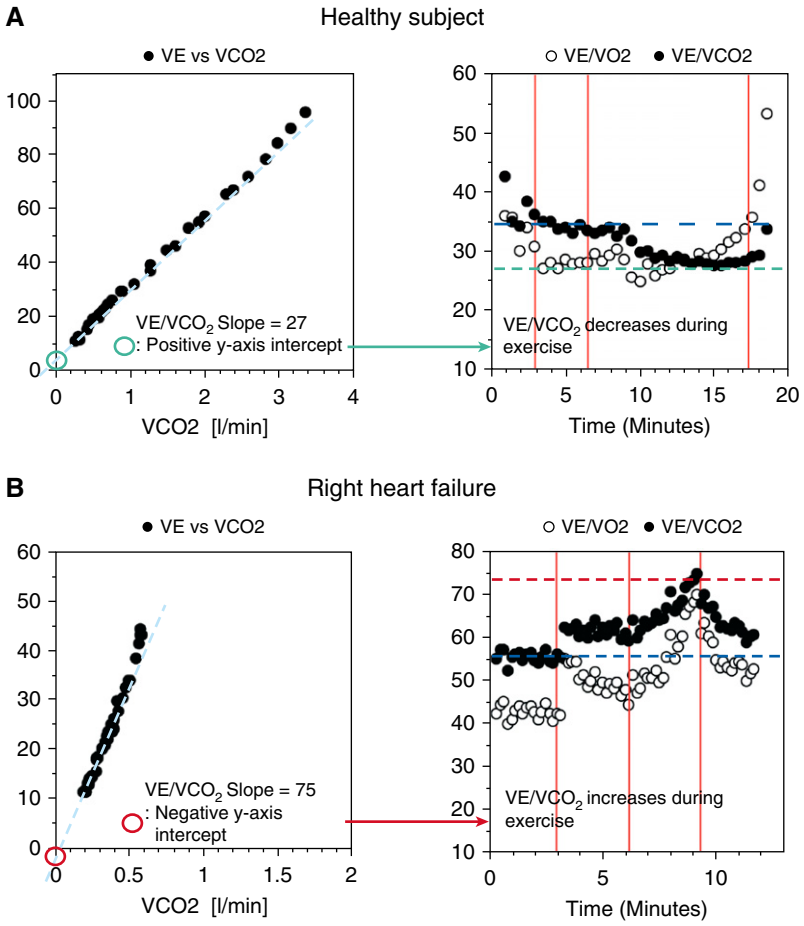

Figure 8. Correlation between the $\dot{V}_E/\dot{V}_{CO_2}$ slope, the *y-axis* intercept, and the $\dot{V}_E/\dot{V}_{CO_2}$ relationship during incremental exercise. Studies of a healthy subject (*A*) and a patient with severe pulmonary arterial hypertension and right-heart failure (*B*). The *vertical red lines* in the right panel column indicate, from left to right, the start of the unloaded pedaling phase, the start of the incremental work rate increase, and the end of the exercise phase, respectively. (*A*) With a positive *y-axis* intercept, the $\dot{V}_E/\dot{V}_{CO_2}$ relationship likely decreases during exercise. (*B*) With a negative *y-axis* intercept, the $\dot{V}_E/\dot{V}_{CO_2}$ relationship likely increases during exercise. The *horizontal blue lines* in the right-hand graphs represent the baseline $\dot{V}_E/\dot{V}_{CO_2}$ ratio at rest. The *horizontal green line* in the upper right-hand graph represents the lowest $\dot{V}_E/\dot{V}_{CO_2}$ ratio that is achieved during exercise (the $\dot{V}_E/\dot{V}_{CO_2}$ ratio decreases during exercise). The *horizontal red line* in the lower right-hand graph represents the highest $\dot{V}_E/\dot{V}_{CO_2}$ ratio that is achieved during exercise the (the $\dot{V}_E/\dot{V}_{CO_2}$ ratio increases during exercise). $\dot{V}_{CO_2}$, $\dot{V}_E$, and $\dot{V}_{O_2}$ are shown in L/min.

established standardized dataset of key parameters as a basis for a structured interpretation. However, many specific questions that arise from basic test interpretation cannot be answered by the nine-panel plot alone. There is an obvious need for extended plots; however, the selection of plots has to be adapted to the clinical questions that have to be answered. An approach to extend plotting of ventilatory efficiency for patients with heart failure has been proposed by Hansen and colleagues (23). Another special graphical application for heart failure and pulmonary hypertension may consist of plotting $\dot{V}_E$ over $P_{ET_{CO_2}}$, which directly reflects hyperventilation and may be useful in several conditions.

As several new technologies are now available for noninvasive cardiac output measurement during exercise, a plot of cardiac output over arteriovenous oxygen difference with iso-$\dot{V}_{O_2}$ lines directly reflects the Fick principle and may give further diagnostic information whether exercise intolerance is rather due to a central limitation (cardiac output) or to a peripheral limitation (skeletal muscle, peripheral oxygen extraction).

The detection of dynamic hyperinflation during exercise is another important clinical question that cannot be answered by the nine-panel plot. Here, recording of flow–volume loops during exercise has become a routine application in the past years.

Conclusions

An optimized graphical display of gas exchange data during exercise is an essential instrument in the interpretation of CPET results. An optimal scaling and styling of the graphs, as well as a standardized plot of the obtained data, may help to substantially improve the efficacy, reliability, and reproducibility of the interpretation process. ■

Author disclosures are available with the text of this article at www.atsjournals.org.

References

1 Beaver WL, Wasserman K, Whipp BJ. On-line computer analysis and breath-by-breath graphical display of exercise function tests. *J Appl Physiol* 1973;34:128–132.
2 Wasserman K, Hansen JE, Sue DY, Whipp BJ. Principles of exercise testing and interpretation, 1st ed. Philadelphia: Lea & Febiger; 1986.
3 Gibbons RJ, Balady GJ, Beasley JW, Bricker JT, Duvernoy WF, Froelicher VF, Mark DB, Marwick TH, McCallister BD, Thompson PD Jr, *et al*. ACC/AHA guidelines for exercise testing: a report of the American College of Cardiology/American Heart Association Task Force on Practice Guidelines (Committee on Exercise Testing). *J Am Coll Cardiol* 1997;30:260–311.
4 Roca J, Whipp BJ, Agustí AGN, *et al*.; ERS Task Force on Standardization of Clinical Exercise Testing. European Respiratory Society. Clinical exercise testing with reference to lung diseases: indications, standardization and interpretation strategies. *Eur Respir J* 1997;10:2662–2689.
5 Rodgers GP, Ayanian JZ, Balady G, Beasley JW, Brown KA, Gervino EV, Paridon S, Quinones M, Schlant RC, Winters WL Jr, *et al*. American College of Cardiology/American Heart Association clinical competence statement on stress testing: a report of the American

College of Cardiology/American Heart Association/American College of Physicians–American Society of Internal Medicine Task Force on Clinical Competence. *J Am Coll Cardiol* 2000;36:1441–1453.
6 Gibbons RJ, Balady GJ, Bricker JT, Chaitman BR, Fletcher GF, Froelicher VF, Mark DB, McCallister BD, Mooss AN, O'Reilly MG, *et al*.; American College of Cardiology/American Heart Association Task Force on Practice Guidelines (Committee to Update the 1997 Exercise Testing Guidelines). ACC/AHA 2002 guideline update for exercise testing: summary article. *Circulation* 2002;106:1883–1892.
7 American Thoracic Society; American College of Chest Physicians. ATS/ACCP statement on cardiopulmonary exercise testing. *Am J Respir Crit Care Med* 2003;167:211–277.
8 Palange P, Ward SA, Carlsen KH, Casaburi R, Gallagher CG, Gosselink R, O'Donnell DE, Puente-Maestu L, Schols AM, Singh S, *et al*.; ERS Task Force. Recommendations on the use of exercise testing in clinical practice. *Eur Respir J* 2007;29:185–209.
9 Mezzani A, Agostoni P, Cohen-Solal A, Corrà U, Jegier A, Kouidi E, Mazic S, Meurin P, Piepoli M, Simon A, *et al*. Standards for the use of cardiopulmonary exercise testing for the functional evaluation of cardiac patients: a report from the Exercise Physiology Section of the European Association for Cardiovascular Prevention and Rehabilitation. *Eur J Cardiovasc Prev Rehabil* 2009;16:249–267.
10 Balady GJ, Arena R, Sietsema K, Myers J, Coke L, Fletcher GF, Forman D, Franklin B, Guazzi M, Gulati M, *et al*.; American Heart Association Exercise, Cardiac Rehabilitation, and Prevention Committee of the Council on Clinical Cardiology; Council on Epidemiology and Prevention; Council on Peripheral Vascular Disease; Interdisciplinary Council on Quality of Care and Outcomes Research. Clinician's Guide to cardiopulmonary exercise testing in adults: a scientific statement from the American Heart Association. *Circulation* 2010; 122:191–225.
11 Guazzi M, Adams V, Conraads V, Halle M, Mezzani A, Vanhees L, Arena R, Fletcher GF, Forman DE, Kitzman DW, *et al*.; European Association for Cardiovascular Prevention & Rehabilitation; American Heart Association. EACPR/AHA scientific statement: clinical recommendations for cardiopulmonary exercise testing data assessment in specific patient populations. *Circulation* 2012;126: 2261–2274.
12 Guazzi M, Arena R, Halle M, Piepoli MF, Myers J, Lavie CJ. 2016 Focused update: clinical recommendations for cardiopulmonary exercise testing data assessment in specific patient populations. *Circulation* 2016;133:e694–e711.
13 Oren A, Sue DY, Hansen JE, Torrance DJ, Wasserman K. The role of exercise testing in impairment evaluation. *Am Rev Respir Dis* 1987; 135:230–235.
14 Wasserman K, Hansen JE, Sue DY, Stringer WW, Sietsema KE, Sun XG, Whipp BJ. Principles of exercise testing and interpretation, 5th ed. Philadelphia: Lippincott Williams & Wilkins; 2012.
15 Wasserman K, Whipp BJ. Excercise physiology in health and disease. *Am Rev Respir Dis* 1975;112:219–249.
16 Beaver WL, Wasserman K, Whipp BJ. A new method for detecting anaerobic threshold by gas exchange. *J Appl Physiol (1985)* 1986;60: 2020–2027.
17 Wasserman K, Cox TA, Sietsema KE. Ventilatory regulation of arterial H(+) (pH) during exercise. *Respir Physiol Neurobiol* 2014;190: 142–148.
18 Ward SA, Whipp BJ. Ventilatory control during exercise with increased external dead space. *J Appl Physiol* 1980;48:225–231.
19 Gargiulo P, Apostolo A, Perrone-Filardi P, Sciomer S, Palange P, Agostoni P. A non invasive estimate of dead space ventilation from exercise measurements. *PLoS One* 2014;9:e87395.
20 Apostolo A, Laveneziana P, Palange P, Agalbato C, Molle R, Popovic D, Bussotti M, Internullo M, Sciomer S, Bonini M, *et al*. Impact of chronic obstructive pulmonary disease on exercise ventilatory efficiency in heart failure. *Int J Cardiol* 2015;189:134–140.
21 Inbar O, Oren A, Scheinowitz M, Rotstein A, Dlin R, Casaburi R. Normal cardiopulmonary responses during incremental exercise in 20- to 70-yr-old men. *Med Sci Sports Exerc* 1994;26:538–546.
22 Gläser S, Koch B, Ittermann T, Schäper C, Dörr M, Felix SB, Völzke H, Ewert R, Hansen JE. Influence of age, sex, body size, smoking, and β blockade on key gas exchange exercise parameters in an adult population. *Eur J Cardiovasc Prev Rehabil* 2010;17:469–476.
23 Hansen JE, Sun XG, Stringer WW. A simple new visualization of exercise data discloses pathophysiology and severity of heart failure. *J Am Heart Assoc* 2012;1:e001883.